23rd ABCM International Congress of Mechanical Engineering
December 6-11, 2015, Rio de Janeiro, RJ, Brazil

NUMERICAL ANALYSIS OF A CONSTANT FLOW IN A DIRECT ABSORPTION SOLAR COLLECTOR FOR WATER HEATING SYSTEMS USING SIMPLE AND PIMPLE ALGORITHMS

Guilherme Biazzi Gonçalves
Department of Mechanical Engineering – Faculty of Engineering – State University of São Paulo (UNESP)
Av. Luiz Edmundo Carrijo Coube s/n, Bauru, São Paulo, Brazil
guibgoncalves.mec@gmail.com

Vicente Luiz Scalon
Department of Mechanical Engineering – Faculty of Engineering – State University of São Paulo (UNESP)
Av. Luiz Edmundo Carrijo Coube s/n, Bauru, São Paulo, Brazil
scalon@feb.unesp.br

Alcides Padilha
Department of Mechanical Engineering – Faculty of Engineering – State University of São Paulo (UNESP)
Av. Luiz Edmundo Carrijo Coube s/n, Bauru, São Paulo, Brazil
padilha@feb.unesp.br

Abstract. *On last decades, the continuous increasing in price and with the perspective for insufficiency of fossil fuels have encouraged research and use of renewable energy. From alternative sources highlighted, the most used on residences is the water heating system with solar flat plate collectors. Another alternative based on this technology is the direct absorption collector, also known as volumetric collector. On this device, the working fluid flows between a black absorber plate on bottom and a glass plate on top. The water flow is heated directly by the sun and indirectly by the absorber plate. This study analyzed the direct absorption collector using two different algorithms, SIMPLE and PIMPLE, in order to verify their effectiveness. For this, it was considered a case where the inflow was constant and equal to 2 L/(min.m²) for three angles, 30°, 45 and 60°. The results obtained by the simulations were compared with theoretical ones and demonstrated a good precision for both algorithms, having relative errors smaller than 2.0% for all the simulations.*

Keywords: *Solar Energy, Direct Absorption Solar Collector, Numerical Analysis, SIMPLE, PIMPLE, OpenFOAM®.*

1. INTRODUCTION

Due to the successive increases in price of fossil fuels and the growing concern of society with the environment, the countries have been investing in development, improvement and implementation of energy generation through renewable sources, which are those derived from naturally replenished resources, like sun, wind and water.

Among all existing forms of energy, the solar is the most abundant on the planet, having a greater energy potential than all other sources together, both renewable and non-renewable. According Thirugnanasambandam et al. (2010), the sun emits a radiation rate of $3.8\text{x}10^{23}$ kW, of which approximately $1.8\text{x}10^{14}$ kW are intercepted by Earth. About 60% of this radiation ($1.08\text{x}10^{14}$ kW) reaches the surface of the planet, while the remainder is reflected into space and absorbed by the atmosphere. If 0.1% of this radiation was converted into other forms of energy with an efficiency of 10%, it would be generated an amount of energy four times greater than the worldwide generation capacity, which was 3000 GW in the date that the article was published.

Besides having all this favorable potential for its implementation, solar energy also has a great variety of systems that can use it, for example, water heating systems, vehicles, solar ponds, air cooling systems, purification and distillation of water, etc.

Shivakumar (1996) describes water heating systems as being constituted, essentially, by a solar collector and a reservoir with internal insulation which are interconnected by tubes. The collector is responsible for picking the solar radiation up which pass through the upper surface made of glass, which also helps to reduce losses by convection and radiation to the environment. Inside the collector, the water can be heated directly, when it flows over an absorbing surface, or indirectly, when it flows inside tubes. The remaining surfaces are insulated in order to reduce losses by heat transfer. At the outlet, the heated water flows into the reservoir where it is stored for use.

Among the existing types of solar collectors, it can be found the direct absorption one, also known as volumetric collector. This apparatus is made of an insulated box with a glass top surface and an absorption plate inside and does not have pipes, it means that the flow occurs between the absorption plate and the glass and the fluid is heated directly.

Usually this type of collector uses nanofluids, a mixture of water and metal nanoparticles, as working fluid, however it increases cost due to the technologies employed for use of nanofluid. Therefore, it seeks, as an alternative, the use of water as working fluid to enable the implementation of this collector in residences.

One of the most practical ways of evaluates a machine or system is through a numerical analysis. According to Chapra and Canale (2010), this type of analysis is the study of algorithms used to solve different problems, which aims to design and analyze techniques in order to provide approximate solutions, but accurate, to problems of difficult or impossible to solve analytics.

To make a numerical analysis it is necessary the use of specific software that are programmed to perform this kind of analysis and solving the problem. Among these software, one that can be named is OpenFOAM (Open Field Operation and Manipulation), which is a CFD (Computational Fluid Dynamics) tool and is used to evaluate situations related with transport phenomena area and its equipment.

This study aims to analyze the accuracy of the results, obtained by numerical analysis, using two algorithms, SIMPLE and PIMPLE, for a constant volumetric flow condition in a direct absorption solar collector using water, as working fluid, in a heating water system using the software OpenFOAM®.

2. LITERATURE REVIEW

2.1 Direct Absorption Solar Collector

Great part of the studies involving direct absorption solar collectors evaluates what is the best kind of nanofluid that can be used, once their high absorb capacity of the solar radiation make them suitable to be used in the equipment. Because of this, few papers relating this type of collector with other fluids, such as water, becoming more common researches comparing conventional fluids and nanofluids in order to demonstrate the superiority of the latter over the former as working fluid for this collector.

Otanicar et al. (2009) performed an experimental work in which they evaluated the absorptive capacity of four fluids: water, propylene glycol, ethylene glycol and Therminol® VP-1. The experiment consisted of locking up a layer, about 1.0 cm thick, of fluid between two layers of Spectrosil® and submits the arrangement to solar radiation in order to measure which wavelengths of light the fluids had more facility to absorb radiation. Results showed that water has the greatest solar absorbing capacity (13.75%) of the studied fluids, however this amount of absorbed energy is low if compared with the nanofluid capacity. As a further conclusion, the authors said that it would be necessary to increase the fluid thickness layer to 1.0 m if they want to reach a rate of 90% of radiation absorption with water.

Saidur el al. (2012) conducted a numerical study to demonstrate the effects of the nanofluids in a direct absorption solar collector, using a mixture of water and aluminum. During the analysis, the authors compared the transmissivity and absorptivity of pure water and the nanofluid. While water is virtually transparent on the visible region of light spectrum, the addition of nanoparticles decreases the transmissivity in 60% for the same collector's area, increasing the fluid's absorptivity, which proves the superiority of nanofluids in relation to other working fluids.

Ladjevardi et al. (2013) performed a similar study using graphite nanoparticles, with different diameters, dissolved in water to create nanofluids with different volumetric concentrations in order to obtain, through numerical and experimental analysis, the best combination of parameters to achieve the greatest effectiveness for the collector and to compare if the approaches made for the numerical model are consistent with the experimental situation. As the study made for Saidur el al., an observation was made about the absorption of the spectrum of light for pure water and nanofluids. The study revealed that for a thickness of 1.0 mm fluid, pure water is able to absorb, approximately, 300 W/m² of solar radiation, while a nanofluid with graphite's volume fraction of 0.00001% can absorb 400 W/m², which is the lowest absorption rate of all the studied nanofluids.

One of the few practical applications of a direct absorption collector using water as working fluid has been designed by McKinney & Purshottam (2011). They designed a collector to heat and sterilize water from a hospital. The equipment developed is composed of an inner plate with slots where the water flows through and two glasses covers, wherein the first is placed over the inner plate and the secondi is positioned above the first cover creating a vacuum between them, which provides thermal insulation. This collector can heat water faster than the normal ones due to direct exposure to sunlight and also can use ther germicidal properties of UV rays to sterilize the water.

2.2 SIMPLE and PISO algorithms

Another important factor that should be taken into regard when performing a numerical analysis is the algorithm that will be used to solve the governing equations of the studied case. In the software used to do this analysis, it can be find an extensive library of algorithms already implemented, so the user has to identify the optimal one for solving the studied problem to begin the simulation. In OpenFOAM®, among the algorithms present in its library, are the SIMPLE (Semi-Implicit Method for Pressure Linked Equations) and PIMPLE (Pressure Implicit Method for Pressure Linked Equations), which is a fusion the algorithms PISO (Pressure Implicit with Splitting of Operator) and SIMPLE, both algorithms are ideal for the analysis of incompressible flows, such as the direct absorption collector. The algorithms use a calculation procedure which involves a pressure-velocity relation to solve the Navier-Stokes equations, wherein the PISO algorithm was formulated from the SIMPLE and reproduces stable results and is more used to find solutions to transient problems.

Nalajala and Kishore (2014) used the SIMPLE algorithm, together with the QUICK (Quadratic Upstream Interpolation for Convective Kinematics) to solve the equations of mas flow and momentum of power-law fluids in which are present impurities bubbles, which causes drag problem in the flow. With respect to the algorithms used, the authors obtained results with only 2.0% of relative error in compare to those found in references, which it makes the algorithms reliable and accurate for cases with Reynolds between 0.1 and 200.

Seif et al. (2010) implemented a PISO algorithm based on a non-conservative approach, to simulate unsteady flow with cavitation, to solve the continuity and Navier-Stokes equations. To prove the algorithm accuracy and efficiency, cavitation simulations were performed on a hydrofoil NACA0015, on a flat plate (two-dimensional analysis) and in a circular disk (three-dimensional analysis) and the results were compared with experimental results already published, which had taken into regard the flow frequency, the pressure distribution, the cavitation vorticity and the cavitation characteristics. The authors concluded that the results generated by the developed algorithm were satisfactory for the studied cases; however they highlighted a need to expand the algorithm to solve more different kind of cavitation problems.

Wanik and Schnell (1988) examined the properties of two PISO algorithms and one SIMPLE algorithm in the moment equations, comparing the computational effort made by each one to reach the same convergence results in two test problems, which considered a flow with and without vorticity in an axisymmetric geometry. The results showed that the PISO algorithms needed less CPU time to solve the test situations, although some tests have showed fluctuations in mesh solutions; the accuracy of PISO are strongly related to the number of iterations, with under-relaxation coefficients and timestep; the SIMPLE was the least effective among the studied algorithms; and the simulations have shown that there are a need for more accurate models for flows with vorticity.

3. METHODOLOGY

The direct absorption collector, represented in Fig. 1, is consisted of an insulated box in which a black absorbing plate is positioned on the inside bottom and a glass plate on tis upper outside surface, and in the space between the plates the working fluid flows, which is, in this study, water. The fluid is heated by radiation through the glass plate and the heat lost from the absorbing plate, in contrast it loses heat by convection to the environment.

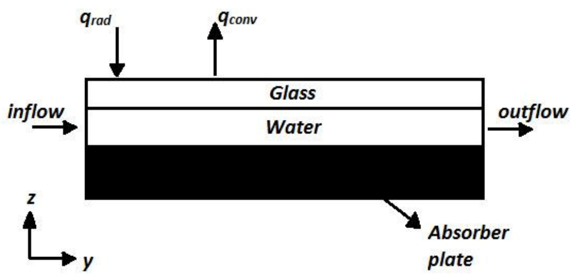

Figure 1. Direct Absorption Collector.

To analyze thermal fluid problems, it is necessary to solve the equations that govern them, which are the equations of continuity, Eq. (1), motion, Eq. (2a), Eq. (2b) and Eq. (2c), and energy, Eq. (3c). These equations are described below for a laminar flow of a Newtonian fluid in the Cartesian coordinates (Bird et al, 1960):

$$\frac{\partial \rho}{\partial t}+\frac{\partial}{\partial x}(\rho v_x)+\frac{\partial}{\partial y}(\rho v_y)+\frac{\partial}{\partial z}(\rho v_z)=0 \tag{1}$$

$$\rho\left(\frac{\partial v_x}{\partial t}+v_x\frac{\partial v_x}{\partial x}+v_y\frac{\partial v_x}{\partial y}+v_z\frac{\partial v_x}{\partial z}\right)=-\frac{\partial p}{\partial x}+\mu\left(\frac{\partial^2 v_x}{\partial x^2}+\frac{\partial^2 v_x}{\partial y^2}+\frac{\partial^2 v_x}{\partial z^2}\right)+\rho g_x \tag{2a}$$

$$\rho\left(\frac{\partial v_y}{\partial t}+v_x\frac{\partial v_y}{\partial x}+v_y\frac{\partial v_y}{\partial y}+v_z\frac{\partial v_y}{\partial z}\right)=-\frac{\partial p}{\partial y}+\mu\left(\frac{\partial^2 v_y}{\partial x^2}+\frac{\partial^2 v_y}{\partial y^2}+\frac{\partial^2 v_y}{\partial z^2}\right)+\rho g_y \tag{2b}$$

$$\rho\left(\frac{\partial v_z}{\partial t}+v_x\frac{\partial v_z}{\partial x}+v_y\frac{\partial v_z}{\partial y}+v_z\frac{\partial v_z}{\partial z}\right)=-\frac{\partial p}{\partial z}+\mu\left(\frac{\partial^2 v_z}{\partial x^2}+\frac{\partial^2 v_z}{\partial y^2}+\frac{\partial^2 v_z}{\partial z^2}\right)+\rho g_z \tag{2c}$$

$$\begin{aligned}\rho c_p\left(\frac{\partial T}{\partial t}+v_x\frac{\partial T}{\partial x}+v_y\frac{\partial T}{\partial y}+v_z\frac{\partial T}{\partial z}\right)=k\left(\frac{\partial^2 T}{\partial x^2}+\frac{\partial^2 T}{\partial y^2}+\frac{\partial^2 T}{\partial z^2}\right)+2\mu\left\{\left(\frac{\partial v_x}{\partial x}\right)^2+\left(\frac{\partial v_y}{\partial y}\right)^2+\left(\frac{\partial v_z}{\partial z}\right)^2\right\}\ldots\\ \ldots+\mu\left\{\left(\frac{\partial v_x}{\partial y}+\frac{\partial v_y}{\partial x}\right)^2+\left(\frac{\partial v_x}{\partial z}+\frac{\partial v_z}{\partial x}\right)^2+\left(\frac{\partial v_y}{\partial z}+\frac{\partial v_z}{\partial y}\right)^2\right\}\end{aligned} \tag{3}$$

where p is the pressure, t is the time, T is the temperature, v is the velocity, g is the gravity, ρ is the fluid density, μ is the fluid dynamic viscosity, c_p is the specific heat and k is the thermal conductivity. The terms in braces on Eq. (3) are associated with viscous dissipation and were neglected for this study, because the flow has a low velocity gradient.

In the analysis, in order to consider the effects of natural convection due to the change in fluid density with temperature variation, it was used the Boussinesq approximation, Eq. (4), which can be determined from the thermal volumetric expansion coefficient definition:

$$\beta=-\frac{1}{\rho}\left(\frac{\partial\rho}{\partial T}\right)_p\rightarrow\beta\approx-\frac{1}{\rho}\frac{\rho_\infty-\rho}{T_\infty-T}$$

$$\left(\rho_\infty-\rho\right)\approx\rho\beta\left(T-T_\infty\right) \tag{4}$$

where β is the thermal volumetric expansion coefficient of the fluid, T_∞ is the ambient temperature and ρ_∞ is the fluid constant density.

In order to verify the accuracy of the results obtained in simulations, it is customary to use theoretical values attained by equations or references so that it can be compared the results and calculated their relative errors. As the objective of this study is to verify the accuracy of two algorithms for the same boundary condition, it was used, as a comparative parameter, the amount of energy rate in the geometry outlet, since the inlet energy and the incident radiation over the plate are constant in both cases studied. To calculate the outlet energy rate, the following sequence of equations was used:

$$\phi=\int_0^{th} v\ L\ dz\rightarrow\phi=v_i\ th\ L;\quad \dot{m}=\rho\phi;$$

$$q''_{rad}wL=\dot{m}c_p\,\Delta T\rightarrow\Delta T=\left(\frac{q''_{rad}wL}{\dot{m}c_p}\right);\ \dot{E}_o=\int_0^{th}\rho c_p vTLdz\rightarrow\dot{E}_o=\dot{m}c_p\left(T_i+\Delta T\right) \tag{5}$$

where ϕ is the volumetric flow of water, v_i is the theoretical inlet velocity of the fluid, th is the geometry thickness, $\dot{m}$ is the mass flow, ΔT is the is the temperature change between the inlet and outlet of geometry, q''_{rad} is the incident radiation gradient, w é the geometry width, $\dot{E}_o$ is the outlet energy rate and T_i is the inlet temperature.

3.1 Boundary Conditions

To perform the analysis, it was created a mesh representing the flow region inside the collector and was set the boundary conditions related to a constant volumetric inflow of 2.0 L/(min.m²) using two different algorithms, SIMPLE and PIMPLE, for verification of which one is more accurate. Although a real collector is subjected to a three-dimensional flow, it was considered, in all cases, a symmetry condition for the x-axis, simplifying the cases to two-dimensional flow in the yz plane.

For all situations, the geometry was the same and it was performed a variation of inclination on 30º, 45º and 60º. It was considered the geometry and physical properties of water are the same. The boundary region was subdivided into inlet, outlet, glass (upper surface) and plate (bottom surface), as shown in Fig. 2.

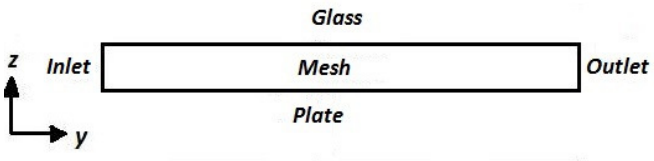

Figure 2. Flow Region Mesh and Boundaries on OpenFOAM®.

3.1.1 Pressure and Velocity

The pressure and velocity boundaries conditions are linked by the equations of continuity and momentum. Therefore, conditions for the velocity field are necessary to use a fitting condition for the pressure field.

At the inlet, to achieve a constant volumetric flow of 2.0 L/(min.m²) on the geometry, it was used a constant velocity of 0.05 m/s in y-direction and the pressure is constant. Considering the outlet boundary region the pressure and velocity values are determinate by the flow development, so a zero gradient condition is used for both fields. On the same way, at the plate and the glass cover no slip condition and no change in the pressure field were adopted.

3.1.2 Temperature

At the inlet surface, the temperature is fixed on 298 K, representing the temperature which the water enters in the collector. The plate was exposed to a constant radiation heat flux of 800 W/m², corresponding to the incident solar radiation over the collector. On glass top a Robin condition, reproducing the convection losses to the environment, was used.

On this surface, it was necessary to calculate the convective coefficient. Considering that the geometry is susceptible to a wind, it was used the equation present in Kalogirou (2009), shown on Eq. (9):

$$h = 8.6\frac{v_w^{0.6}}{L^{0.4}} \tag{6}$$

where h is the convective coefficient, L is the length of the collector and v_w is the wind velocity.

The convection losses were converted on a gradient temperature boundary condition using Eq. (7):

$$\frac{\partial T}{\partial z} = -\left(\left(T_s - T_\infty \right) * \left(\frac{h}{k} \right) \right) \tag{7}$$

where $\partial T/\partial z$ is the temperature gradient in the z-direction, and T_s is the surface temperature.

4. RESULTS AND DISCUSSION

For numerical simulations and equations described in the previous section, the geometry dimensions, the physical properties of water, the initial data, and their measurement units, are presented in Tab. 1, remembering that the heat transfer coefficient was determined from Eq. (6) using a wind velocity of 5.0 m/s.

Before perform the collector analysis, a mesh size teste was done. This test was performed with ten different mesh sizes to select that can reproduce the results with good accuracy and time. The results are shown in Fig. 3.

It can be noted by the graphs on Fig.3 that the lower is the mesh product of $\Delta y*\Delta z$, the lower is the relative error of the simulations results, but it takes more computational time to achieve the specified tolerance. Considering the meshes analyzes, it was chosen the on with the $\Delta y*\Delta z$ ration equal to $3x10^{-8}$ m², because it showed accurate results in an adequate computational time.

Figure 4 shows the velocity profile at the inlet, middle and outlet regions of z-axis on the geometry for the 30° angle using both algorithms. At all the positions analyzed, the velocity profiles present similar behaviors. The same behavior, are not showed but, can be found on 45° and 60° results.

Table 1.Geometry Dimensions, Water Physical Properties and Initial Data

Dimensions/Property/Constants	Value	Unit
Length (L)	1.5	[m]
Width (w)	$1.0x10^{-3}$	[m]
Thickness (th)	$1.0x10^{-3}$	[m]
Density (ρ)	988.1	[kg/m³]
Dynamic Viscosity (μ)	$5.47x10^{-4}$	[N.s/m²]
Kinematic Viscosity (ν)	$5.53x10^{-7}$	[m²/s]
Thermal VolumetricExpansion Coefficient (β)	$4.51x10^{-4}$	[K^{-1}]
Specific Heat (c_p)	4181.0	[J/kg.K]
Thermal Condutivity (k)	0.644	[W/m.K]
Heat Transfer Coefficient (h)	19.21	[W/m².K]
Gravity (g)	9.81	[m/s²]
Atmospheric Pressure (p_0)	$101.325x10^{3}$	[Pa]
Ambient Temperature (T_∞)	300	[K]

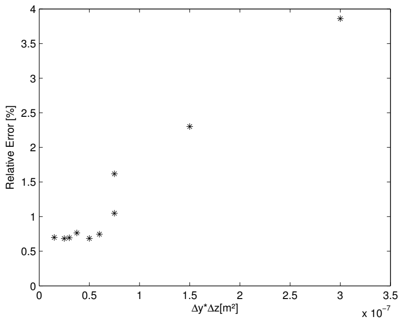

(a)

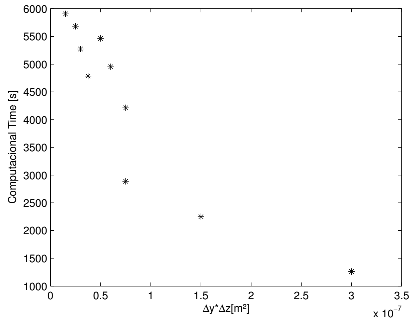

(b)

Figure 3. Results from Mesh Test (a) accuracy (b) elapsed time

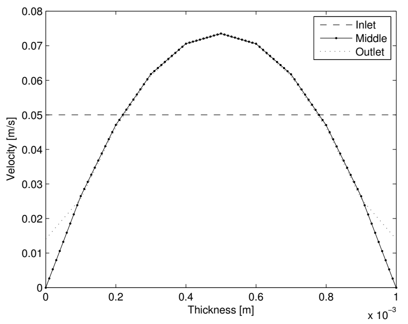

(a)

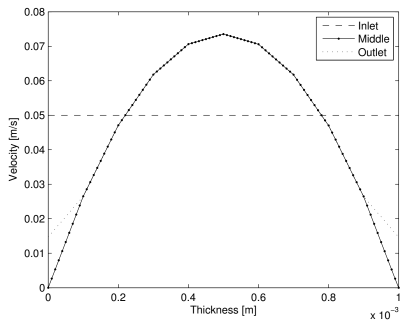

(b)

Figure 4. Velocity Profiles for 30° (a) SIMPLE, (b) PIMPLE.

Figure 5 illustrates the results obtained for the outlet energy rate for all three angles analyzed by the algorithms. The theoretical value, represent by the setpoint curve, was obtained from Eq. (8), totaling 62.8 W, with light difference of expected output energy.

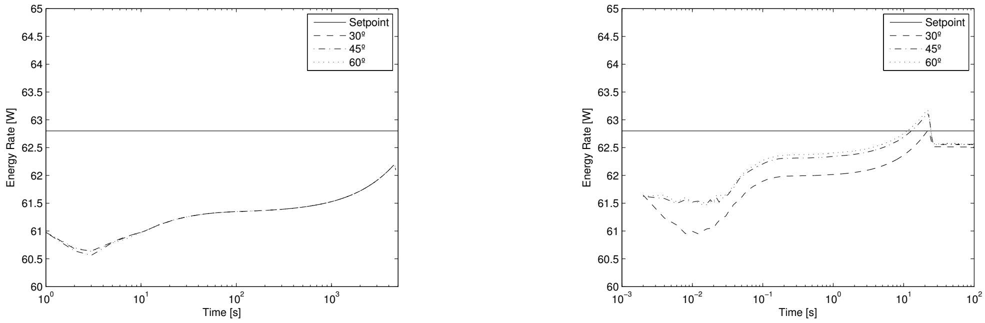

(a) (b)

Figure 5. Output energy for 30°, 45° and 60°, for (a) SIMPLE algorithm and (b) PIMPLE algorithm.

It can be noticed through the graphics presented in Fig. 5 that the outlet energy rate results for the three inclinations studied by the PIMPLE algorithm and are similar closed to the setpoint. Despite not having the same accuracy, the results obtained by SIMPLE also converge to a value close to the reference. The results of both algorithms showed good accuracy, since the relative errors for all simulations are less than 2.0%. As expected, it is noted in the second chart that in the final simulation time interval the three curves are straight, demonstrating that system is already stable solution.

Figure 6 compares the results obtained by the algorithms for convective heat transfer, per unit of area, at the geometry upper surface (glass) at the final simulation time, while Fig. 7 represents the temperature for the same surface and conditions. The results obtained for 45º and 60º with PIMPLE were physically inconsistent and are not shown.

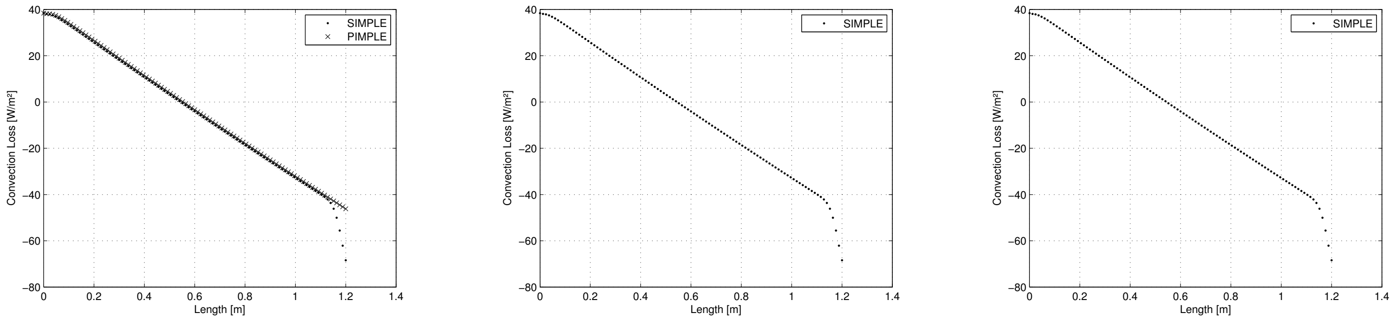

(a) (b) (c)

Figure 6. Comparison of heat losses by convection between the algorithms, (a) 30°, (b) 45° and (c) 60°.

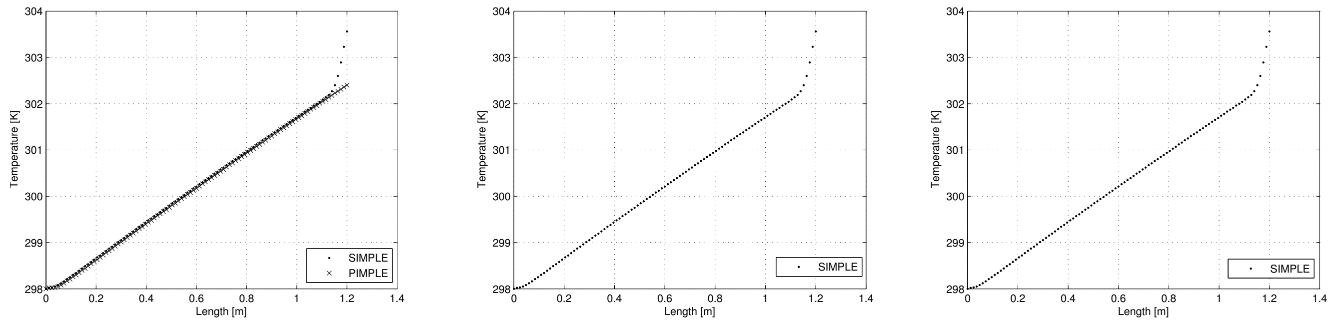

(a) (b) (c)

Figure 7. Comparison of temperature on top surface between the algorithms, (a) 30°, (b) 45° and (c) 60°.

The curves behavior in Fig. 6 and Fig. 7 show that, there is a heat gain by convection at the beginning of the geometry, since the environmental temperature (300 K) is higher than the glass surface temperature. This behavior continues until the length of approximately 0.55 m. From this point and on, the glass temperature is higher than the environmental and, thereby, the water loses heat by convection.

It is also notice that in the length ending, from 1.39 approximately, light differences between the heat flux obtained values by SIMPLE for cases and PIMPLE for 30º, confirming the accuracy for both algorithms showed in the outlet energy analysis.

5. CONCLUSIONS

The study aimed to investigate the behavior of SIMPLE and PIMPLE algorithms in numerical analysis of a direct absorption solar collector using a constant flow of 2 L/(min.m²) at the inlet and determine the accuracy and efficiency of both algorithms.

In the outlet energy rate analysis the PIMPLE algorithm obtained results closer to the theoretical values than those obtained by SIMPLE, but both are accurate and efficient for the case studied. Relative errors observed in the six simulations were less than 2.0% and considered quite acceptable for numerical analyzes.

As regards to heat losses by convection to the ambient, the results showed a similar behavior for both algorithms on the 30º case and only for SIMPLE on the 45º and 60º cases in almost the entire length of the geometry, showing small differences in the last 0.1 m, which was already indicated by the outlet energy values. These changes could be caused by differences observed in velocity profile in outlet surface. It is worth to note that until the length of 0.55 m the glass gain heat by convection because the surface temperature is smaller than the ambient.

Thus, it can be concluded that both algorithms can be used for the case studied, as they have accurate and reliable results with a slight advantage to the PIMPLE. For future work, the authors intend to use more diverse boundary conditions, so that can be possible to determine the algorithms behavior and identify which is most recommended for each situation. Additional investigations for verifying the causes of differences in outlet velocity profile will be also done.

6. REFERENCES

BIRD, R.B.; STEWART, W.E.; LIGHTFOOT, E.N. *Transport Phenomena*. University of Wisconsin, Madisson, 1960.

CHAPRA, S.C; CANALE, R.P. *Numerical Methods for Engineers and Scientists*. 6ª Ed. McGraw Hill, New York, 2010.

INCROPERA, F.P.; DeWITT, D.P.; BERGMAN, T.L.; LAVINE, A.S. *Fundamentals of Heat and Mass Transfer*. 6th Edition, Wiley, United States, 2007.

KALOGIROU, S. *Solar Energy Engineering: Processes and Systems*. Elsevier,1st Ed., London, 2009.

LADJERVARDI, S.M.; ASNAGHU, A.; IZADKHAST, P.S.; KASHANI, A.H. *Applicability of graphite nanofluids in direct solar energy absorption*. Solar Energy, Vol. 94, pp. 327-334, 2013.

NALAJALA, V.S.; KISHORE, N. *Drag of contaminated bubbles in power-law fluids*. Colloids and Surfaces A: Physicochemical and Engineering Aspects, nº 443, pp. 240-248, 2014.

OTANICAR, T.P.; PHELAN, P.E.; GOLDEN, J.S. *Optical properties of liquids for direct absorption solar thermal energy system*. Solar Energy, Vol. 83, pp. 969-977, 2009.

SAIDUR, R.; MENG, T.C.; SAID, Z.; HASANUZZAMAN, M.; KAMYAR, A. *Evaluation of the effect of nanofluid-based absorbers on direct solar collector*. International Journal of Heat and Mass Transfer, Vol. 55, pp. 5899-5907, 2012.

SEIF, M.S.; ASNAGHI, A.; JAHANBAKHSH, E. *Implementation of PISO algorithm for simulationg unsteady cavitating flows*. Ocean Engineering, nº 37, pp. 1321-1336, 2010.

SHIVAKUMAR, A.R. *A value addition to a modern house design: an integrated domestic solar water heater*. Energy for Sustainable Development, Vol. 3, nº 1, pp. 54-58, 1996.

THIRUGNANASAMBANDAM, M.; INIYAN, S.; GOIC, R. *A review of solar thermal technologies*. Renewable and Sustainable Energy Reviews, Vol. 14, pp. 312-322, 2010.

WANIK, A.; SCHNELL, U. *Some Remarks on the PISO and SIMPLE algorithms for steady turbulent flow problems*. Computers & Fluids, Vol. 17, nº 4, pp. 555-570, 1989.

7. RESPONSIBILITY NOTICE

The authors are the only responsible for the printed material included in this paper.